Article

Waterjet Cutting Vibration Analysis of Difficult to Cut Materials

Michał Leleń *, Katarzyna Biruk-Urban, Jerzy Józwik

Posted Date: 14 August 2023

doi: 10.20944/preprints202308.0968.v1

Keywords: abrasive water-jet cutting; difficult-to-cut materials; vibration measurements

Article

Waterjet Cutting Vibration Analysis of Difficult to Cut Materials

Michał Leleń *, Katarzyna Biruk-Urban and Jerzy Józwik

Faculty of Mechanical Engineering, Lublin University of Technology, ul. Nadbystrzycka 36, 20-618 Lublin, Poland; m.lelen@pollub.pl (M.L.); k.biruk-urban@pollub.pl (L.B.-U.); j.jozwik@pollub.pl (J.J.)

* Correspondence: m.lelen@pollub.pl, k.biruk-urban@pollub.pl

Abstract: The cutting of difficult-to-machine materials, including their preconditioning, often requires specialised tools and machinery. An alternative processing technology can be cutting materials with a water jet. From the initial stage, the selection of appropriate technological parameters will influence what further finishing treatments will be applied. Vibrations occurring during this process can negatively affect the quality of the cutting edges and surfaces. Therefore, this study analysed vibrations during water-jet cutting with variable technological parameters (speed v_{fi} and pressure p_i). To measure the vibrations, a three-axis accelerometer from SEQUOIA was used in water-jet cutting of three materials: aluminum alloy, titanium alloy, and steel. Based on the study, it was found that the maximum value of vibration amplitude reaches the lowest value of vibration acceleration for aluminum alloy (not exceeding 5 m/s^2), regardless of the value of pressure during the cutting process. This, taking into account the material properties, indicates that aluminum alloy is the material most susceptible to the cutting process while maintaining a high quality of the cutting surface. Significantly higher values of vibration acceleration amplitude (reaching up to 60 m/s^2) during cutting were registered for steel and titanium alloy in all zones and phases of the process (entry zone, cutting zone, and exit zones).

Keywords: abrasive water-jet cutting; difficult-to-cut materials; vibration measurements

1. Introduction

The constitution of machine part geometries has been evolving rapidly for many years with the emergence of new technologies. Water-jet machining (AWJ) of materials, which involves the use of high-pressure water along with the addition of an abrasive, has become a popular method for shaping machine parts in various industries around the world [1]. Waterjet cutting is a unique technology that uses a high-pressure water jet mixed with abrasives to cut a variety of materials, including composites, glass, steel and multilayer structures [2]. The flexibility of this technology has made it widely used in the aerospace, automotive and construction industries [3].

Optimal selection of cutting parameters is essential to ensure the stability and reliability of the cutting process, as well as to achieve a high-quality cutting surface. However, achieving these optimal cutting parameters can be a technological challenge, often due to process instability and insufficient data needed to stabilise the process [4, 5]. Consequently, there is a need to develop strategies for monitoring and controlling the material cutting process with the primary objective of enhancing the cutting process quality and, subsequently, attaining the best possible cutting surface quality [6, 7].

Cutting materials through water-jet processing offers several advantages compared to other cutting methods like laser cutting or plasma cutting [8]. These benefits include the ability to cut through materials with diverse properties, even those that are challenging to cut using traditional methods, and the creation of a small heat-affected zone, leading to reduced thermal deformation. This is particularly crucial for precision cutting applications [9, 10]. Additionally, in many cases, especially for rough machining, water-jet cutting eliminates the need for additional operations like milling, resulting in time and cost savings [11]. Consequently, water-jet cutting has gained popularity as a surface treatment technology, surpassing other cutting methods like laser cutting and plasma cutting [12, 13]. Various researchers have employed both vibration and acoustic emission for real-

 doi:10.20944/preprints202308.0968.v1

time monitoring of the AWJ (abrasive water-jet) process. According to the literature [14], the first group of methods focuses on tracking the vibration signal parameters of the process itself and the working elements, and their impact on the final product's quality. The second group is concerned with diagnostics and condition monitoring of machine components based on the acoustic emission signal, aiming to identify the sources of the emission. As for the first category, most experimental studies involve the extraction of synthetic indicators, such as the root mean square (RMS) of the monitored signal, which has proven to be sensitive to the process and its parameters, as well as the condition of working components [15].

One of the disadvantages of the abrasive-water jet (AWJ) cutting process is its inherent instability, leading to vibrations that negatively impact the quality of the cutting edge and surface. However, monitoring these vibrations during the cutting process presents an opportunity to enhance the stability and reliability of the process, consequently influencing the quality of the surface and edges after cutting [16,17]. Experimental studies have demonstrated that vibrations can be effectively identified using an accelerometer attached to the workpiece being measured [18]. This approach was also utilised in the study [19]. and it can be employed in further experimental investigations on measuring vibrations during WaterJet abrasive jet cutting of various materials, including composites, glass, and steel [20,21].

The use of a non-invasive vibration sensor to monitor vibration during abrasive waterjet cutting offers several advantages. First and foremost, it provides a practical and non-intrusive solution for a vibration monitoring system, which is crucial for ensuring the stability and reliability of the cutting process [22]. Additionally, this approach enables real-time vibration monitoring, providing valuable feedback that can be utilised to adjust cutting parameters and improve cutting quality [23].

In the AWJM (Abrasive Water Jet Machining) process, high-speed abrasive particles suspended in a water jet impact the workpiece surface, leading to vibrations in the workpiece and generating acoustic signals [24]. Researchers, such as Peržel et al. [25]. have analysed vibrations occurring during the cutting of stainless steel. In their study, the variable parameter was the abrasive mass flow rate, set at 250 and 400 g·min-1 (with a constant feed rate). The study measured amplitudes and frequency spectra to establish the relationship between the input factors of the AWJM process and the emission of vibrations and acoustic signals. Tyč et al. [26] investigated the cutting process of hard-to-machine materials (RSt 37-2 steel) of various thicknesses during AWJ. The study involved using three piezoelectric accelerometers as the core of a vibration monitoring station. The tests revealed a strong correlation between the root mean square (RMS) value of the signal and the feed rate. An increase in feed rate caused a corresponding increase in the RMS value, depending on the direction of vibration measurement by the accelerometer. Krenický and Rimár [27] in their research, measured vibrations to analyse the technological parameters of AWJM cutting. They employed nozzle stabilization and a specially designed workpiece clamping system to reduce vibrations. Another study by Karminis-Obratanski et al. [28] aimed to determine whether vibration measures could be utilised to monitor the efficiency of the AWJM process. The study concluded that there was no direct relationship between process efficiency and vibration amplitude. However, they observed an increase in average vibration amplitude with the depth and width of the cut.

Zagórski et al. in [29] on the basis of a study on the effect of varying parameters of water-jet cutting of cast aluminum, concluded that the parameter that has a significant effect on the surface roughness after cutting is the feed speed v_f.

An analysis of the literature indicates that there is still a gap in research on the relationship between the vibrations occurring during water-water jet cutting and the cutting surface quality of various materials. Therefore, it is important to properly select the machining parameters to achieve the lowest possible vibration in order to achieve the desired edge and cutting surface quality of the materials under analysis.

2. Materials and Methods

The research was conducted using an Eckert Combo water-jet cutting machine, which features a modern CNC controller ECK 872. This controller is operated by Windows XP and is linked to a

Preprints (www.preprints.org) | NOT PEER-REVIEWED | Posted: 14 August 2023 doi:10.20944/preprints202308.0968.v1

touch screen, facilitating seamless interaction between the machine and the operator and enabling efficient control of the cutting process. The machine is equipped with an Ethernet connection and a USB interface, simplifying the transfer of programmed programs and leading to time-saving and work optimisation.

The Eckert WaterJet Combo cutting machine, presented in Figure 1, is equipped with a high-pressure UHDE pump capable of generating a maximum pressure of up to 350 MPa. With this pump, the machine is capable of efficiently cutting various materials up to 150 mm thick, making it a versatile cutting tool.

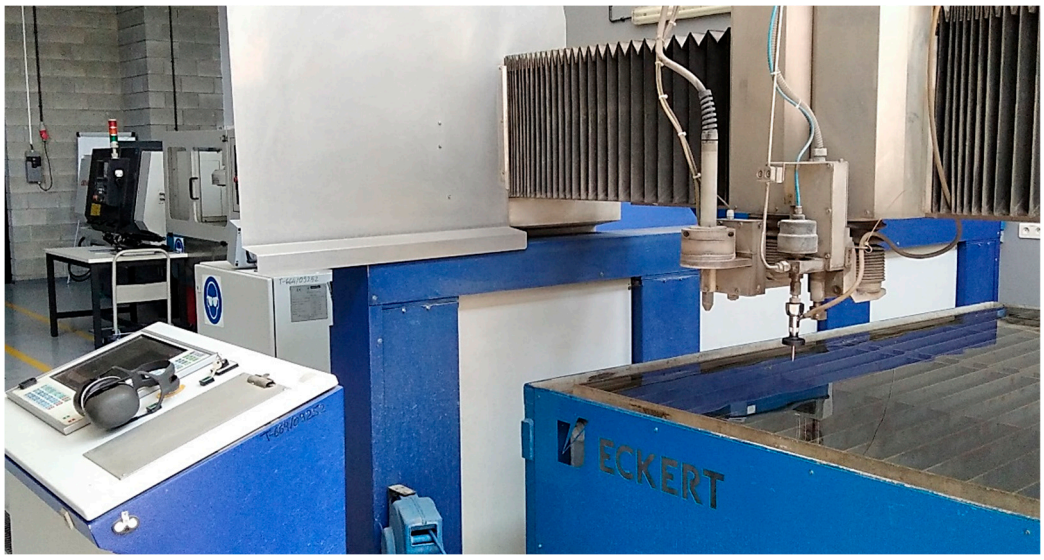

Figure 1. Eckert WaterJet COMBO portal cutting machine.

Samples made of titanium alloy, aluminum alloy and steel were used in the study. Titanium Grade 5 (Ti-6Al-4V) is the most widely used titanium alloy, which is used in a wide range of industrial applications (from aerospace to medicine). It consists of 90% titanium, 6.4% aluminum, 4.1% vanadium and other elements. Table 1 shows its chemical composition.

Table 1. Chemical composition of titanium alloy Ti-6Al4V [% mas.]

Al	V	C	Fe	O_2	N_2	H_2	Ti
6.4	4.1	0.1	0.16	0.18	0.01	0.03	Rest

Alloy 2024 is an aluminum-copper alloy that is widely used in the aerospace industry. It is known for its excellent strength and hardness, making it ideal for manufacturing parts that must withstand heavy loads, such as aircraft wings and fuselages. Table 2 shows the chemical composition of aluminum alloy 2024.

Table 2. The chemical composition of Al2024 alloy [% mas.].

Al	Cu	Mg	Mn	Fe	Si	Zn	Ti	Cr
93.5	3.8–4.9	1.2–1.8	0.3–0.9	⩾0.5	⩾0.5	⩾0.25	⩾0.15	⩾0.1

S235JR is a grade of structural steel extensively used in various sectors of the economy, including the engineering industry and construction. This type of steel is favored as a structural material due to its widespread availability and excellent mechanical properties. Notably, S235JR steel is well-regarded for its good weldability and formability, making it an ideal choice for structural applications. Additionally, its relatively soft nature makes it easy to cut and machine. For detailed information on the chemical composition of S235JR steel, please refer to Table 3.

Preprints (www.preprints.org) | NOT PEER-REVIEWED | Posted: 14 August 2023 doi:10.20944/preprints202308.0968.v1

Table 3. Chemical composition of S235JR steel [% mas.].

C	Mn	Cu	Al	Mo	Si	P	S	Fe
0.16	0.4	0.03	0.04	0.03	0.016	0.05	0.017	Rest

The study used test specimens with dimensions: 200 x 80 x 15 mm. The height of the sample, and at the same time the depth of the cut, was 15 mm. In the course of the experiment, vibration measurements were carried out during the cutting of the samples with a water-abrasive jet, with varying process parameters.

The main component of the measurement station shown in Figure 2 for monitoring vibrations during the cutting process was a SeTAC three-axis accelerometer from SEQUOIA. The Sequoia sensor, was placed at a fixed distance from the cutting edge of 100 mm.

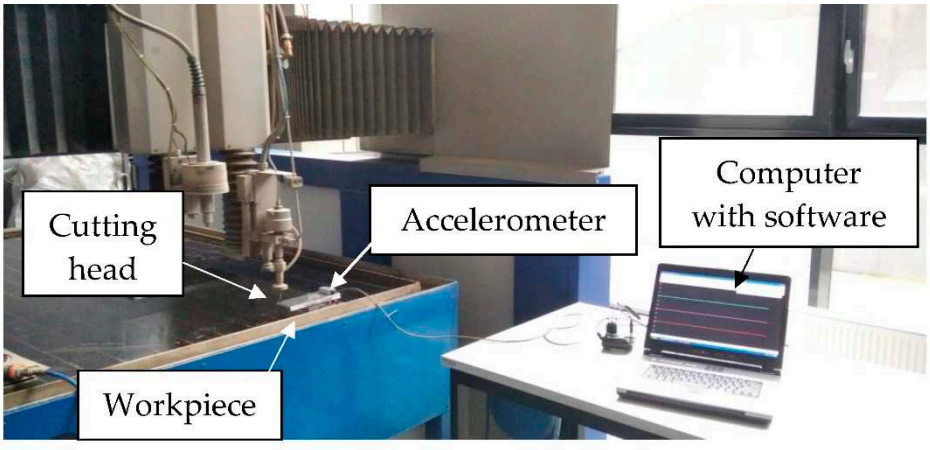

Figure 2. Test stand for vibration measurement.

The SeTAC (Sequoia) system consists of a specialised sensor that measures acceleration, which is connected to a high-precision transducer of the collected signals. The task of the transducer is to convert the measured acceleration into an electrical signal, which is then analysed and interpreted by a computer system. The computer used in this system is equipped with SeTAC software, used to process and display the measurement results, as well as analyse them. Pictures of the measurement station are shown in Figure 3..

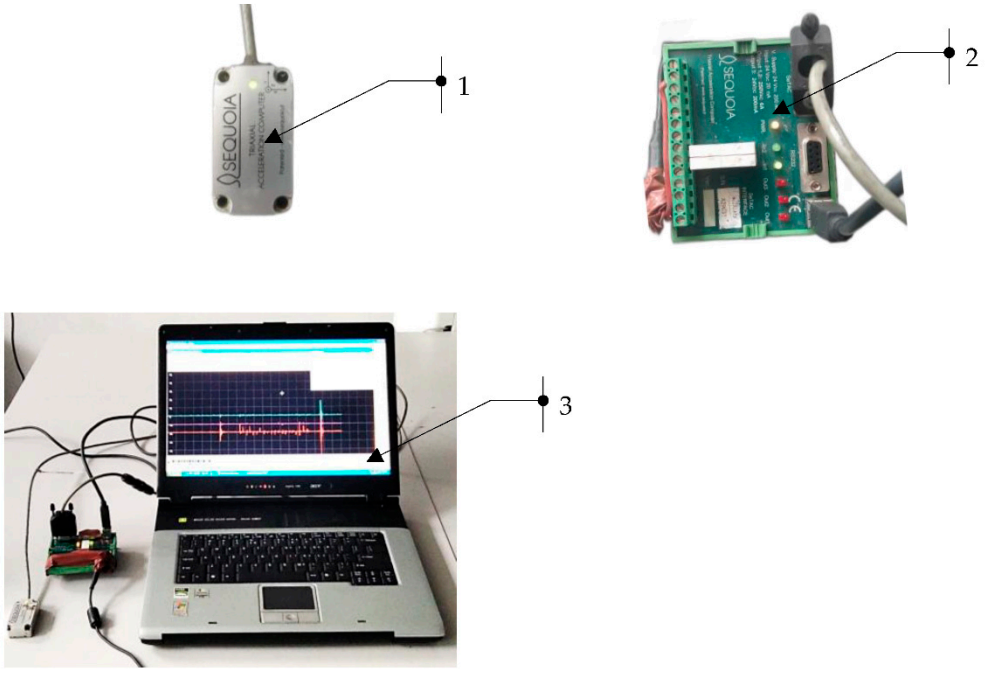

Preprints (www.preprints.org) | NOT PEER-REVIEWED | Posted: 14 August 2023 doi:10.20944/preprints202308.0968.v1

Figure 3. Measurement stand: 1 - vibration sensor, 2 - signal transducer, 3 - computer for signal analysis.

The software used in the research facilitates real-time vibration monitoring to optimise the cutting process by minimising vibrations. To ensure precise measurements, a vibration sensor was securely attached to the object using beeswax. This ensures a stable connection between the sensor and the material, allowing for accurate transmission of the measured vibrations during the entire measurement process. Consequently, the sensor remains firmly attached to the measuring point throughout the tests.

During all the conducted tests, the position of the sensor was rigorously maintained in the same place and at a constant distance from the edge of the material being cut. This consistent positioning is vital for obtaining high-quality data, enabling accurate and objective evaluation of the vibrations produced during cutting.

The primary objective of the research was to evaluate the influence of input technological parameters on vibrations during the cutting process of various materials. The key parameters analysed during the study were the working pressure p [MPa] and the cutting speed v_f [mm/min]. These parameters are critical in water-jet cutting technology as they significantly impact cutting efficiency and quality [10]. The research focused on analyzing the effect of technological cutting conditions on the value of acceleration and their amplitude a [m/s²].

In the experiment, as shown in Figure 4, the researchers employed a research plan with input variables that were modified to observe their effect on the cutting process. The process variables included the working pressure p_i [MPa] and the cutting speed v_{fi} [mm/min]. These variables were systematically altered to study their impact on the cutting process and vibrations.

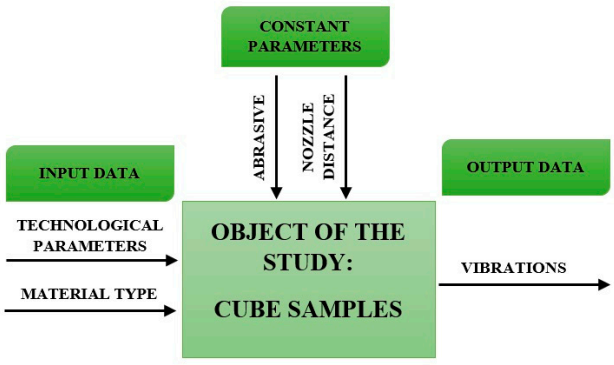

Figure 4. Research model.

Table 4 shows a summary of the constant technological parameters of cutting, i.e. the mass flow rate of abrasive m_a [g/s], the distance of the nozzle from the material being cut h [mm] and the type of abrasive.

Table 4. Summary of constant technological parameters.

Technological Parameters	
Abrasive material	Garnet 80 mesh
Nozzle length	100 mm
Mass flow rate	8 g/s
Distance from the material being cut	3 mm

In order to thoroughly investigate the effect of varying process parameters (shown in Table 5), a series of experiments were conducted with different combinations of input parameter values. Four different working pressures (p_1 = 350 MPa, p_2 = 300 MPa, p_3 = 250 MPa, p_4 = 200 MPa) and four different feed speed (v_{f1} = 30 mm/min, v_{f2} = 40 mm/min, v_{f3} = 50 mm/min, v_{f4} = 60 mm/min) were used. In

Preprints (www.preprints.org) | NOT PEER-REVIEWED | Posted: 14 August 2023 doi:10.20944/preprints202308.0968.v1

addition, three construction materials were used: steel S235JR (b_1), aluminum alloy Al2024 (b_2) and titanium alloy Ti-6Al4V (b_3).

Table 5. Summary of the variable technological parameters.

No.	Material	Pressure p_i [MPa]	Feed speed v_{fi} [mm/min]
1	steel, b_1, aluminum alloy, b_2, titanium alloy, b_3	350	30
2			40
3			50
4			60
5		300	30
6			40
7			50
8			60
9		250	30
10			40
11			50
12			60
13		200	30
14			40
15			50
16			60

3. Results and discussion

Figure 5 presents a schematic of the experimental tests conducted, illustrating the key elements used in the process. The diagram depicts the nozzle utilised for cutting through the test material. The nozzle moved at a predetermined feed speed v_f relative to the material being cut, represented as b. This controlled movement of the nozzle allowed for precise management of the cutting parameters, avoiding the influence of uncontrolled fluctuations in the displacement rate. Vibrations generated during the cutting process were recorded by the vibration sensor, indicated as 1 in the diagram. The vibration signal transducer, marked as 2, converted the recorded sensor signal into a format interpretable by the computer system, designated as 3. This conversion allowed for data interpretation and enabled rapid analysis to correct the technological parameters of the experiment. To ensure the stability and repeatability of the process and eliminate additional factors that could impact the test results, the cut sample was securely clamped to the table. This stable mounting of the sample was crucial for consistent and reproducible results. The vibration sensor was fixed at a fixed distance of $a = 100$ mm from the cutting points. This standardised distance ensured that the vibrations were consistently measured at the same location, enabling accurate comparisons and reliable analysis of the data.

Preprints (www.preprints.org) | NOT PEER-REVIEWED | Posted: 14 August 2023 doi:10.20944/preprints202308.0968.v1

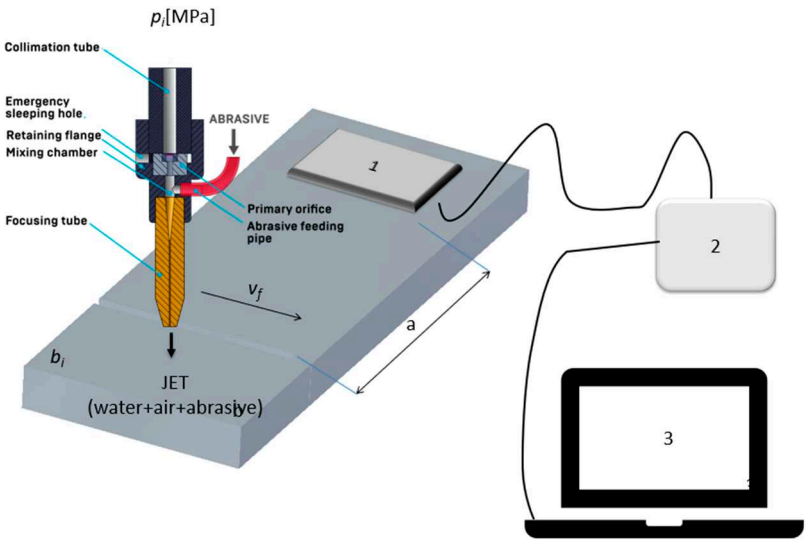

Figure 5. Schematic of the test stand.

Figure 6 shows an example of vibration waveforms for steel (v_f = 30 mm/min, p = 350 MPa). The presented waveforms marked with different colours correspond to the signals recorded in each axis: X, Y, Z. From the example waveform, it can be seen that there are three main zones in the water-wall cutting process: the entry zone (1), the zone of stabilised cutting process (2) and the exit zone (3). In the entry zone, the increase in vibration is due to the impact of the water-abrasive jet on the surface of the water and coming into contact with the surfaces of the material being cut (zone marked 1). The effect of this, due to the strong force interaction, is an increase in the amplitude of vibration, the stabilization of which occurs only in the second zone. The second zone marked No. 2- of the stabilised cutting process - in the full material, is characterised by a stabilised value of vibrations. During the exit of the jet from the cut material (zone three marked No. 3), an increase in vibrations is again noticeable, resulting from the exit of the jet from the material and the jet hitting the water surface again. The initial (4) and final (5) signal waveforms mark the period before the cutting process begins and ends.

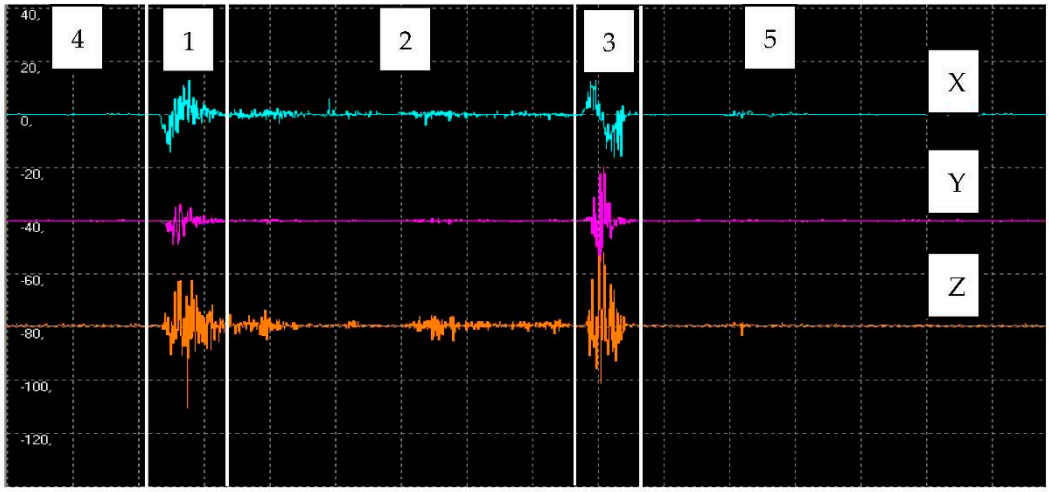

Figure 6. Time course of vibration with marked cutting areas: entry zone (1), stabilised cutting zone (2) and exit zone (3).

This article presents only selected vibration time waveforms describing the studied phenomenon.

Figures 7–9 showcases examples of vibration waveforms for the X-axis, Y-axis, and Z-axis recorded during the cutting process of aluminum alloy (Al2024) at specific technological parameters:

Preprints (www.preprints.org) | NOT PEER-REVIEWED | Posted: 14 August 2023 doi:10.20944/preprints202308.0968.v1

pressure p_1=350 MPa, and speed v_2=40 mm/min. The presented time courses of vibration acceleration reveal three characteristic zones occurring during the cutting process. In the X-axis, the maximum vibration value of 20.7 m/s² occurs in the entrance zone. In the Y-axis, the maximum vibration amplitude of 22.6 m/s² is observed in the exit zone. Meanwhile, in the Z-axis, the highest vibration with an amplitude of 21.4 m/s² occurs in the entrance zone. The increase in vibration amplitude in the exit zone can be attributed to the exit of the water-abrasive stream from the material and its impact on the surface of the water table. In the stabilised zone, which is characterised by comparable vibration values in all axes, the maximum value of vibration does not exceed 5 m/s². This suggests that the cutting process stabilises in this zone, leading to reduced vibrations and ensuring a higher quality of the cutting surface.

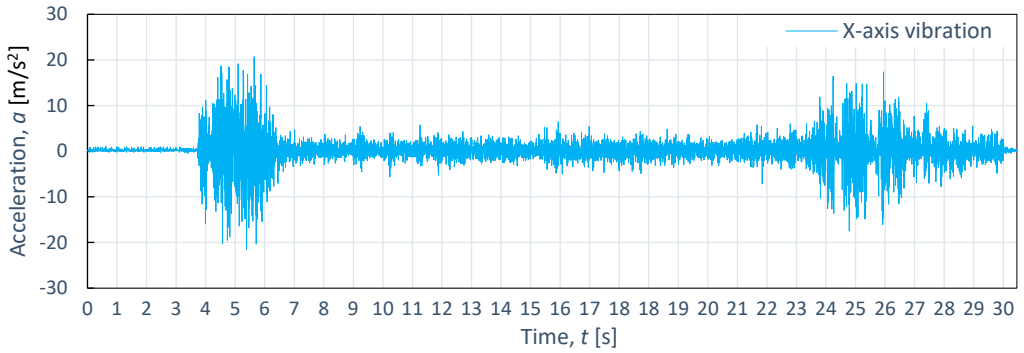

Figure 7. Example of time course of changes in acceleration $a(t)$ (vibration) in the X axis for aluminum alloy Al2024, obtained at: p_1=350 MPa, v_2= 40 mm/min.

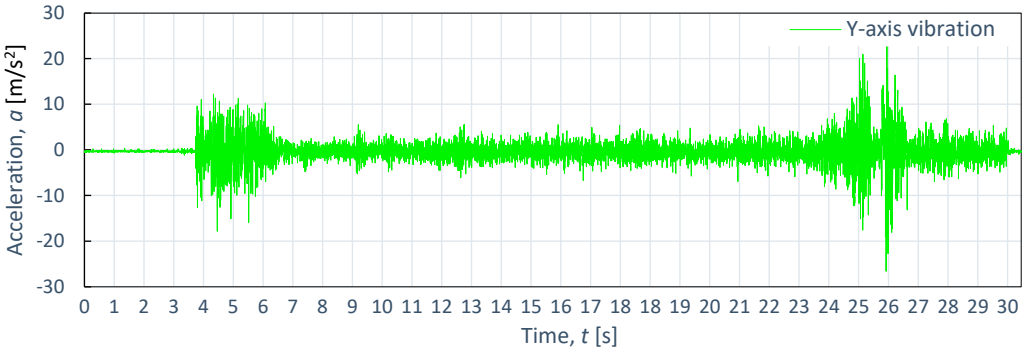

Figure 8. Example of time course of changes in acceleration $a(t)$ (vibration) in Y axis for aluminum alloy Al2024, obtained at: p_1=350 MPa, v_2= 40 mm/min.

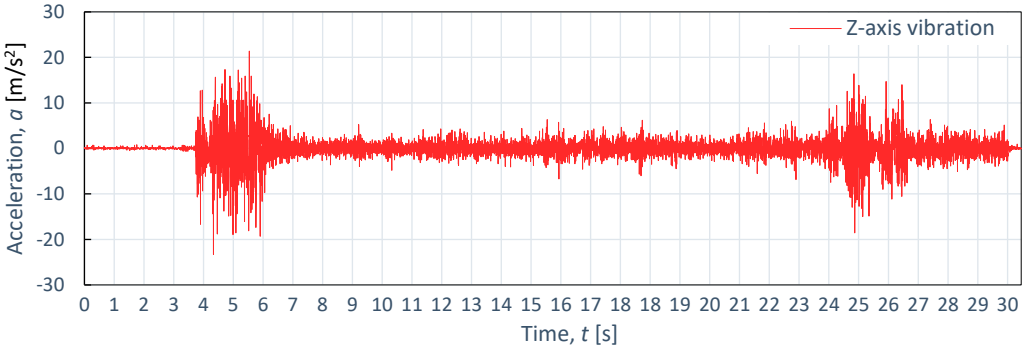

Figure 9. Example of time course of changes in acceleration $a(t)$ (vibration) in Z axis for aluminum alloy Al2024, obtained at: p_1=350 MPa, v_2= 40 mm/min.

Preprints (www.preprints.org) | NOT PEER-REVIEWED | Posted: 14 August 2023 doi:10.20944/preprints202308.0968.v1

Figures 10–12 also display example vibration time waveforms in three axes (X, Y, Z) for S225JR steel at process parameters of pressure p_1=350 MPa and speed v_2=40 mm/min. Figure 10 presents the vibration signal for the X-axis, Figure 11 for the Y-axis, and Figure 12 for the Z-axis. An analysis of Figures 10-12 reveals that, similar to the case of aluminum alloy (Al2024), three characteristic zones can be distinguished for S225JR steel: the entry zone (1), the stabilised cutting zone (2), and the exit zone (3). The entry zone (1) covers the period from the start of the cutting process until the water jet comes into contact with the edges and surfaces of the material being cut. In this zone, significant changes in the waveform of the vibration signal are observed. Notably, this zone is longer for the S225JR steel being cut compared to the vibration time waveform for Al2024 aluminum alloy, despite maintaining the same technological cutting parameters. The zone of the stabilised cutting process refers to cutting through the full material, where, according to the study, no significant deviations in the values of the vibration amplitude were observed. This zone is shorter with respect to Al2024 aluminum alloy. The exit zone is characterised by an increased value of vibration amplitude.

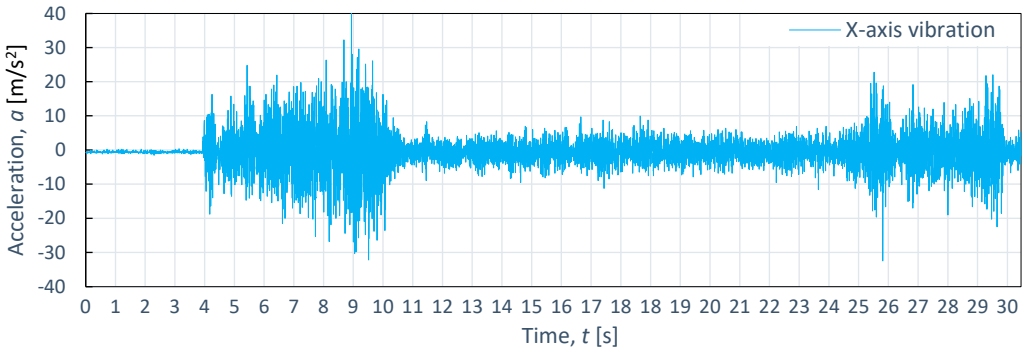

Figure 10. Example of time course of changes in acceleration $a(t)$ (vibration) in X axis for S235JR steel, obtained at: p_1=350 MPa, v_2= 40 mm/min.

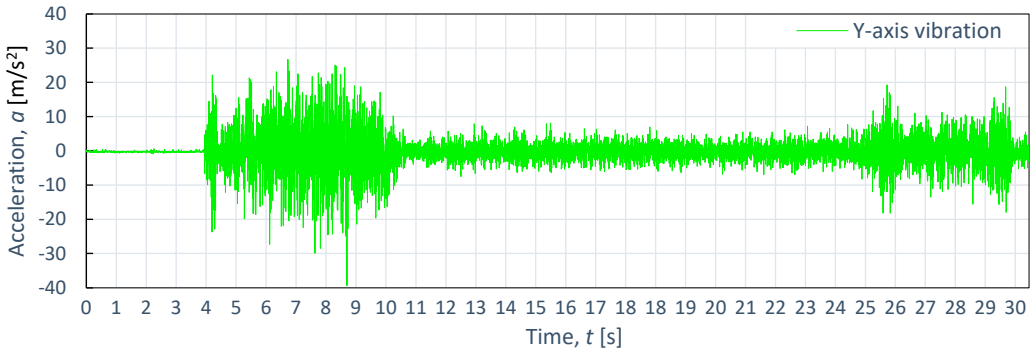

Figure 11. Example of time course of changes in acceleration $a(t)$ (vibration) in Y axis for S235JR steel, obtained at: p_1=350 MPa, v_2= 40 mm/min.

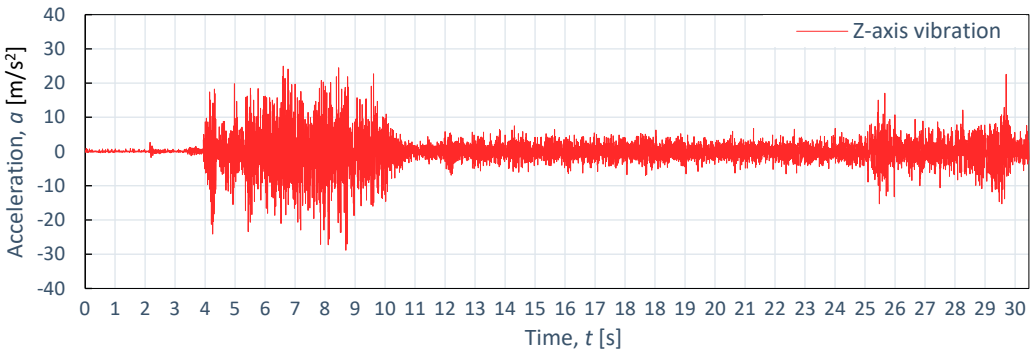

Preprints (www.preprints.org) | NOT PEER-REVIEWED | Posted: 14 August 2023 doi:10.20944/preprints202308.0968.v1

Figure 12. Example of time course of changes in acceleration $a(t)$ (vibration) in Z axis for S235JR steel, obtained at: p_1=350 MPa, v_2= 40 mm/min.

During the cutting of S225JR steel, the entry zone is characterised by a longer duration compared to the exit zone observed during the cutting of aluminum alloy. Additionally, significant differences were noted in vibration values between the entry zone and the exit zone. In the exit zone, the vibration values were considerably smaller compared to the entry zone.

In the entry zone, the highest vibration amplitudes were observed in the X-axis, reaching as high as 42.3 m/s². For the Y-axis in the same area, the highest vibration amplitude was 39.3 m/s², while for the Z-axis, the highest value of vibration amplitude was 28.8 m/s². Conversely, in the stabilised zone, the vibration amplitudes were similar for all axes, not exceeding 10 m/s². When compared to the results obtained for aluminum alloy, the percentage increase in vibration values for S225JR steel was 104.35% for the X-axis, 73.89% for the Y-axis, and 34.58% for the Z-axis, respectively.

The process of cutting steel involves the interaction of many factors, including material characteristics and technological cutting parameters.

Figures 13–15 shows the results of the time course of vibrations during the cutting of titanium alloy Ti-6Al4V. Recorded during the cutting process with the same technological parameters as aluminum alloy and steel. The course of vibration characteristics during the cutting of titanium alloy Ti-6Al4V was characterised by the fact that in the initial input zone for the X-axis the vibrations were 167.45% larger with respect to the vibrations during the cutting of aluminum alloy and 31% larger compared to the vibrations recorded during the cutting process of steel. Their maximum amplitude value was 55.4 m/s².

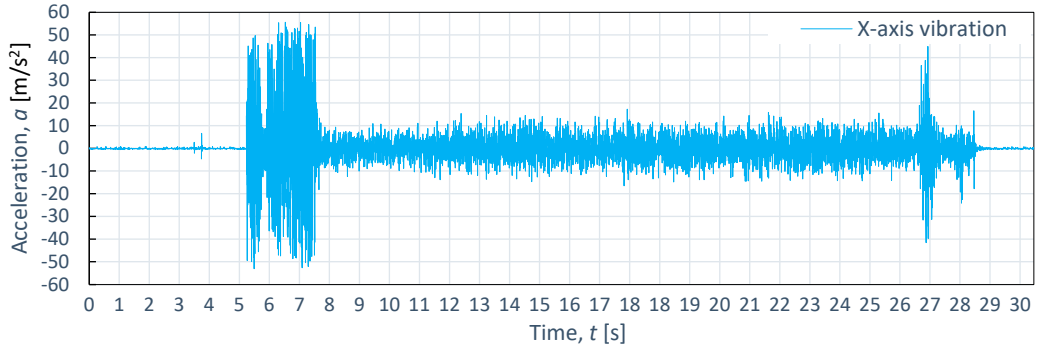

Figure 13. Example of time course of changes in acceleration $a(t)$ (vibration) in X axis for titanium alloy Ti-6Al4V, obtained at: p_1=350 MPa, v_2= 40 mm/min.

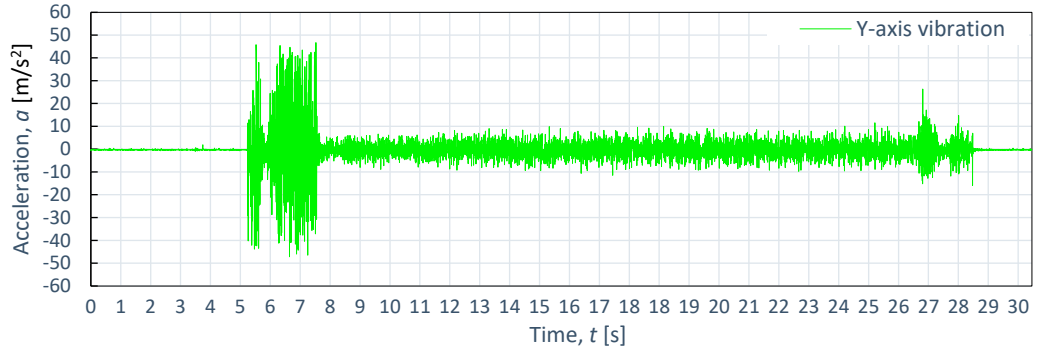

Figure 14. Example of time course of changes in acceleration $a(t)$ (vibration) in Y axis for titanium alloy Ti-6Al4V, obtained at: p_1=350 MPa, v_2= 40 mm/min.

Preprints (www.preprints.org) | NOT PEER-REVIEWED | Posted: 14 August 2023 doi:10.20944/preprints202308.0968.v1

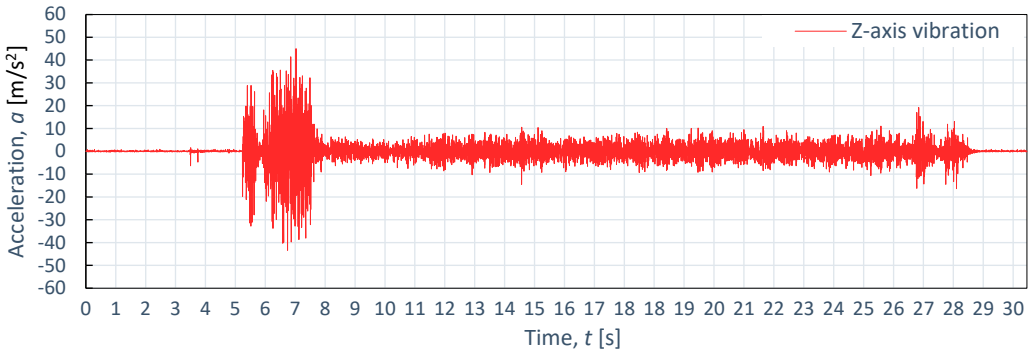

Figure 15. Example of time course of changes in acceleration $a(t)$ (vibration) in Z axis for titanium alloy Ti-6Al4V, obtained at: p_1=350 MPa, v_2= 40 mm/min.

Similarly, in the stabilised zone, compared to steel and aluminum alloy, the average vibration values were 5 m/s² higher. The exit zone was shorter than in the case of steel.

The comparative evaluation of vibration time characteristics during the cutting of aluminum alloy Al2024, steel S235JR, and titanium alloy Ti-6Al4V was performed based on constructed graphs depicting the dependence of maximum acceleration (a_{max}) as a function of pressure (p_i) for four tested feed speeds (v_i) for each of the selected materials subjected to the cutting process (b_i). The analysis covered four different feed speeds: v_1=30 mm/min (Figure 16), v_2=40 mm/min (Figure 17), v_3=50 mm/min (Figure 18), and v_4=60 mm/min (Figure 19).

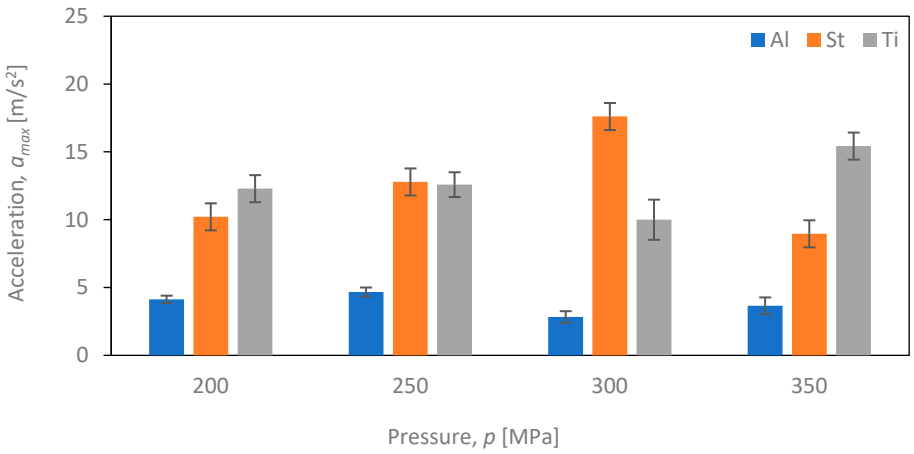

Figure 16. Summary of maximum a_{max} values for cutting speed v_1= 30 mm/min at different p_i pressures of different b_i materials.

Preprints (www.preprints.org) | NOT PEER-REVIEWED | Posted: 14 August 2023 doi:10.20944/preprints202308.0968.v1

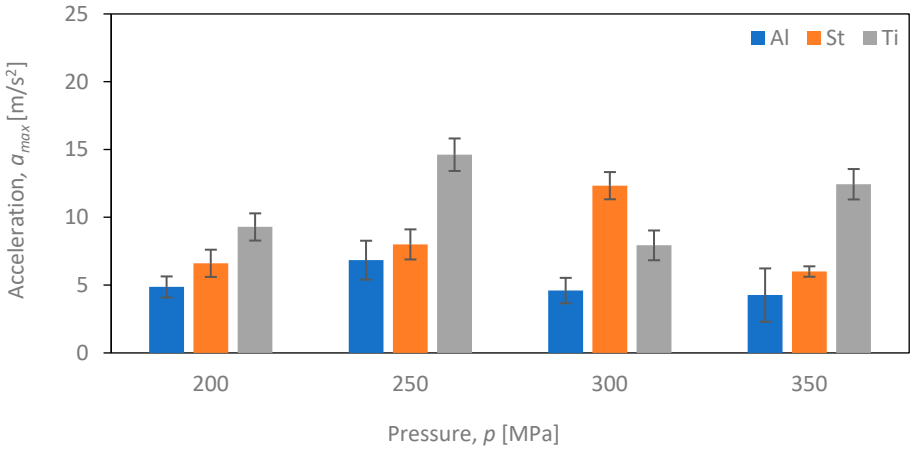

Figure 17. Summary of maximum a_{max} vibration amplitude values for velocity v_2= 40 mm/min at different p_i pressures for different b_i materials.

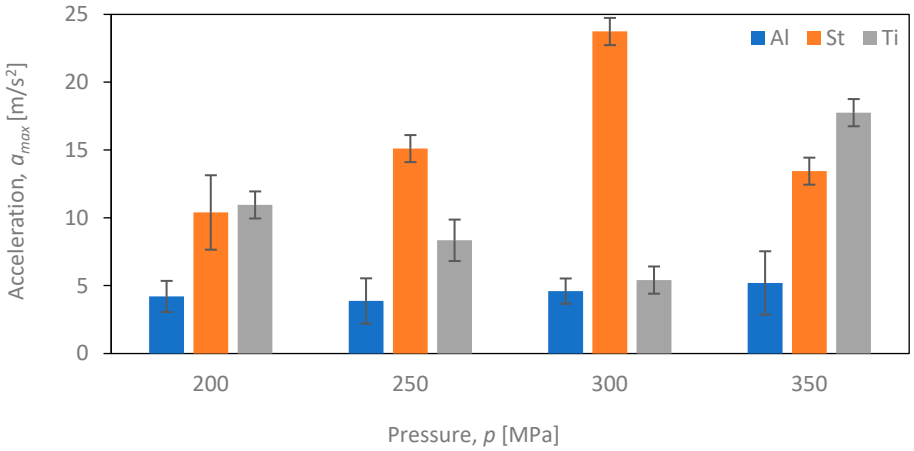

Figure 18. Summary of maximum a_{max} for velocity v_3= 50 mm/min at different p_i pressures for different b_i materials.

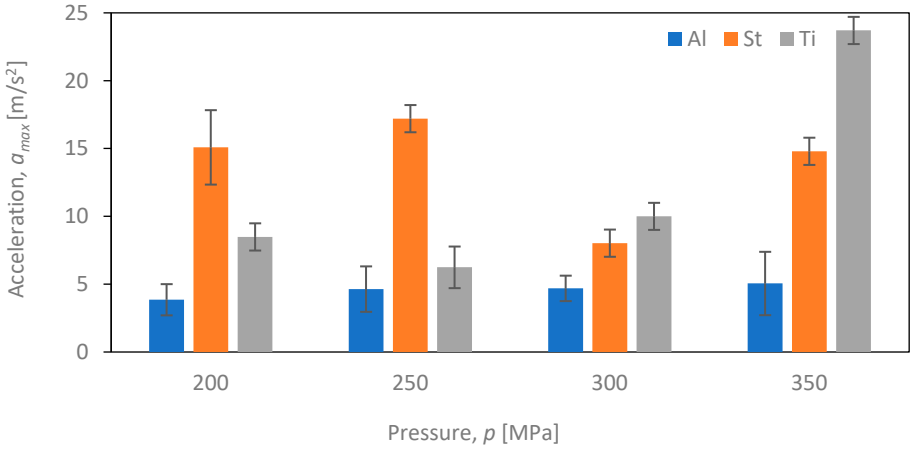

Figure 19. Summary of maximum a_{max} values for velocity v_4= 60 mm/min at different p_i pressures for different b_i materials.

 doi:10.20944/preprints202308.0968.v1

Figure 16 provides a comparison of the maximum vibration amplitude as a function of pressure (p) for speed v_1 and the three materials analysed, namely aluminum alloy Al2024, steel S235JR, and titanium alloy Ti-6Al4V.

Figure 16 illustrates that the maximum value of vibration amplitude for aluminum alloy Al2024 remains consistently low (not exceeding 5 m/s²) regardless of the p_i pressure value. Notably, Al2024 aluminum alloy has the lowest density among the three analysed materials. On the other hand, for S235JR steel, there is a significant correlation between the p_i pressure value and the maximum vibration values. An increase in pressure up to 300 MPa results in a proportional increase in vibration intensity when cutting S235JR steel. However, at a pressure of 350 MPa, there is a decrease in the maximum vibration amplitude for this material. In the case of titanium alloy, the highest values of maximum vibration amplitude were recorded at a pressure of 350 MPa, reaching 15.4 m/s², while the lowest values were observed at a pressure of 300 MPa, measuring 10 m/s². The decrease in vibration amplitude was 35.6%.

Figure 17 shows the dependence of the maximum values of vibration amplitude (a_{max}) for the feed speed v_2 = 40 mm/min.

Similar to the case of velocity v_1, the maximum value of vibration amplitude reaches its lowest value for aluminum (not exceeding 6.8 m/s²) regardless of the pressure value (p). On the other hand, the highest value of maximum vibration amplitude was achieved when cutting titanium alloy Ti-6Al4V at a pressure of p=250 MPa, measuring 14.6 m/s², which is 114.7% higher than the maximum vibration amplitude obtained for aluminum alloy Al2024. A similar trend is observed when cutting S235JR steel - the values of maximum vibration amplitude increase with increasing pressure up to 300 MPa, after which, at the maximum pressure of 350 MPa, the maximum vibration amplitude decreases to 6 m/s².

Figure 18 displays the values of maximum vibration amplitude for a feed speed of v_3=50 mm/min.

For steel, a trend was observed for the maximum value of vibration amplitude to increase with increasing pressure up to a value of 300 MPa. This increase assumes a maximum value at the same point among all analysed velocities and reaches a maximum value of vibration amplitude of 23.7 m/s² just at v_3. At 350 MPa, there is a decrease in vibration. The lowest values of vibration amplitude were achieved, as in the case of other feed speed, for aluminum alloy Al2024 not exceeding 5 m/s². Analysing the results for titanium alloy Ti-6Al4V, we can see that the lowest values of vibration amplitude were recorded at 300 MPa for each feed speed (v_1 =30 mm/min, v_2 =40 mm/min, v_3 =50 mm/min, v_4 = 60 mm/min). The lowest value of vibration amplitude was 17.7 m/s².

In Figure 19, the maximum vibration values for v_4=60 mm/min are presented.

At the highest feed speed v_4, the trend characteristic of lower feed speed for S235JR steel was not observed. Instead, there was no linear increase in vibration amplitude values up to a pressure of 300 MPa, and the maximum vibration amplitude values for this material were reached at the lowest pressures of 200 and 250 MPa, measuring 15 m/s² and 17.2 m/s², respectively. The lowest value of maximum vibration amplitude for steel was 17.2 m/s² at 250 MPa. Conversely, the highest value of maximum vibration amplitude of 23.7 m/s² was achieved for titanium alloy Ti-6Al4V at the highest pressure, which was 282.26% higher than the value obtained for titanium alloy Ti-6Al4V at 250 MPa.

In the case of aluminum alloy Al2024, the value of maximum vibration significantly deviates from the values for the other materials regardless of the adopted feed speed vf. This observed trend is consistent for all combinations of technological parameters, primarily due to the lack of a noticeable increase in vibration values when cutting Al2024 aluminum alloy.

These results highlight the importance of selecting the proper feed speed v_{fi} to obtain optimal vibration amplitude results. A feed speed v_{fi} that is too low can result in a slow and inefficient cutting process, while a feed speed that is too high can lead to increased vibration. By finding the optimal feed speed v_{fi} for each material (b_i), it is possible to achieve a more efficient and high-quality cutting process.

Below, Figures 21 and 22 shows a_{max} vibration amplitudes for three different materials: aluminum alloy, steel and titanium alloy. By analysing the vibration amplitudes and stabilization times in the X,Y,Z axes, one can better understand the physical basis of the cutting process under

Preprints (www.preprints.org) | NOT PEER-REVIEWED | Posted: 14 August 2023 doi:10.20944/preprints202308.0968.v1

certain conditions. This information is very valuable for optimising cutting parameters and selecting the right materials for a given application.

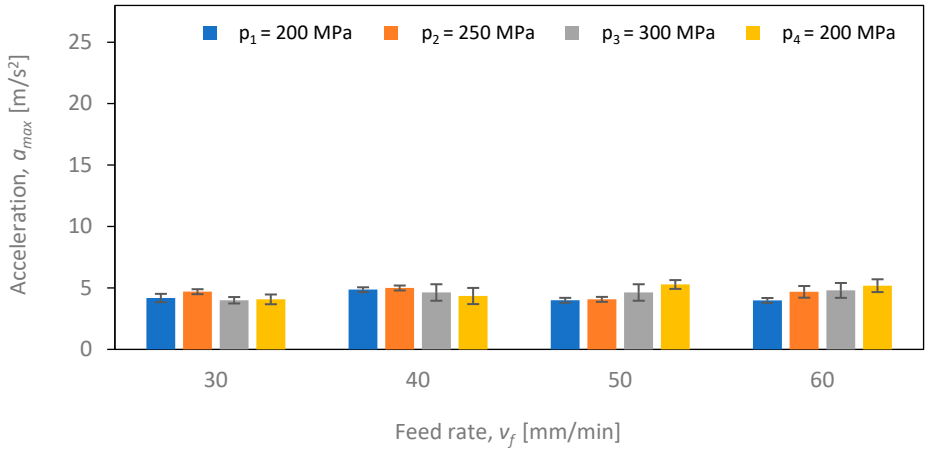

Figure 20. The course of changes in the amplitude value of a_{max} for defined technological parameters of cutting: pressure p_1 = 200 MPa, p_2 = 250 MPa, p_3 = 300 MPa, p_4 = 350 MPa and cutting speed v_1 = 30 mm/min, v_2 = 40 mm/min, v_3 = 50 mm/min, v_4 = 60 mm/min for aluminum alloy Al2024.

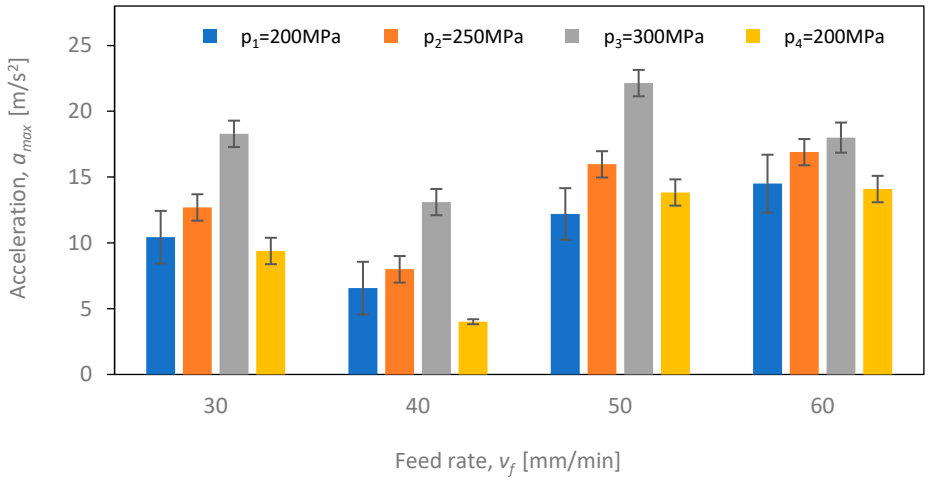

Figure 21. The course of changes in the amplitude value of a_{max} for defined technological parameters of cutting: pressure p_1 = 200 MPa, p_2 = 250 MPa, p_3 = 300 MPa, p_4 = 350 MPa and cutting speed v_1 = 30 mm/min, v_2 = 40 mm/min, v_3 = 50 mm/min, v_4 = 60 mm/min for S235JR steel.

Preprints (www.preprints.org) | NOT PEER-REVIEWED | Posted: 14 August 2023 doi:10.20944/preprints202308.0968.v1

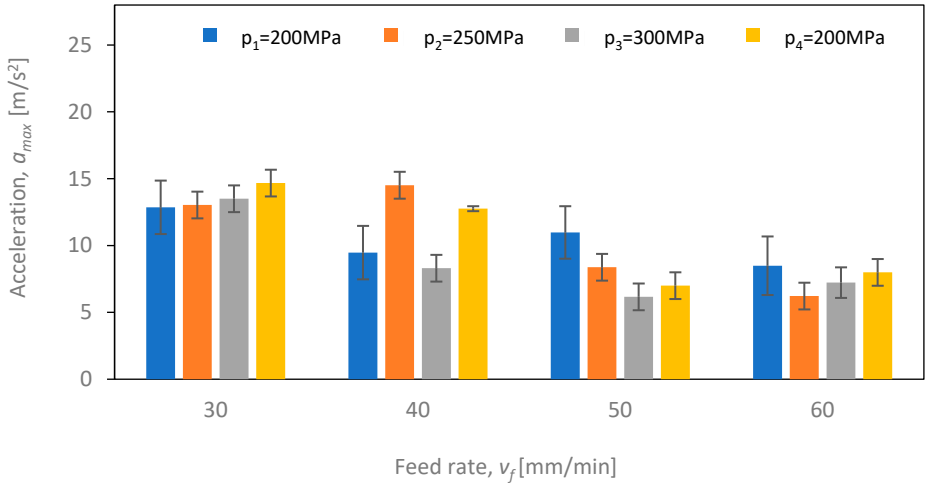

Figure 22. The course of changes in the amplitude value of a_{max} for defined technological parameters of cutting: pressure p_1 = 200 MPa, p_2 = 250 MPa, p_3 = 300 MPa, p_4 = 350 MPa and cutting speed v_1 = 30 mm/min, v_2 = 40 mm/min, v_3 = 50 mm/min, v_4 = 60 mm/min for titanium alloy Ti-6Al4V.

Based on the analysis of the obtained experimental data and the determined estimates (Figure 20) during the cutting of Al2024 aluminum alloy, it is evident that the lowest values of vibration amplitude were recorded, regardless of the values of the technological parameters of cutting. The amplitude values of maximum vibrations (a_{max}) do not exceed 5 m/s². Throughout the adopted range of technological cutting parameters, the cutting process of the aluminum alloy remained stable. This stability can be attributed to several factors. Firstly, Al2024 aluminum alloy is characterised by the lowest density among the tested materials, allowing it to absorb a large amount of energy during the cutting process. Additionally, the alloy's low hardness positively influences the machining process by minimizing the level of vibrations generated. These combined characteristics of Al2024 aluminum alloy contribute to the overall stability of the cutting process and result in low vibration amplitudes.

When analysing the experimental data recorded during the cutting of steel (Figure 21), an increase in the value of vibration amplitude was observed compared to the cutting process of Al2024 aluminum alloy. Comparing the maximum vibration amplitude value for steel, which is 22.4 m/s² at pressure p_3=300 MPa and feed speed v_f=50 mm/min, with the same parameters for Al2024 aluminum alloy, a noticeable 380% increase in vibration amplitude is evident. Additionally, for the first three pressure values: p_1=200 MPa, p_2=250 MPa, and p_3=300 MPa, a linear increase in vibration amplitude is noticeable. However, when the pressure changes to 350 MPa, there is a significant decrease in amplitude for all values of the feed speed v_f, amounting to as much as 75% at a feed speed of 60 mm/min. Steel is the material for which the water-jet cutting process implies the highest values of vibration amplitude. The highest value of vibration amplitude was achieved at a pressure of 300 MPa and feed speed v_f=50 mm/min, reaching 22.1 m/s².

In the case of water-abrasive cutting of titanium alloy Ti-6Al4V (Figure 22), a significant decrease in vibration amplitude values can be observed for feed speed v_f=50 mm/min and v_f=60 mm/min amounting to 97.1% and 75% at 350 MPa with respect to the results obtained for S235JR steel. The highest values of vibration amplitude occur for the smallest value of feed speed v_{fi} and do not exceed 15 m/s². As the feed speed v_{fi} increases, a decrease in vibration amplitude is observed. This trend is preserved for all values of pressure p_i.

In conclusion, the analysis of peak acceleration values in the AWJM process has provided valuable insights into the causal relationships between the technological conditions of the cutting process and the parameters describing the levels of mechanical vibrations generated during hydro-abrasive cutting of various materials. This understanding of the phenomena occurring during hydro-abrasive machining can significantly impact the improvement of the efficiency and effectiveness of

 doi:10.20944/preprints202308.0968.v1

the AWJM process across a wide range of materials. Industries such as aerospace and biomedical, where hydro-abrasive machining is indispensable, stand to benefit greatly from these findings.

The obtained results offer valuable information for optimising cutting conditions tailored to specific materials, while also aiding in the reduction of vibrations and their amplitudes to enhance the overall quality and efficiency of the cutting process. By implementing the knowledge gained from this research, it is possible to advance the capabilities of the AWJM process, making it a more reliable and efficient method for cutting various materials in critical industries

4. Conclusions

The conducted experimental research focused on evaluating the influence of three key technological parameters of waterjet cutting, namely working pressure *pi*, feed speed v_f, and material type (S235JR steel, Al2024 aluminum alloy, and Ti-6Al4V titanium alloy), on the amplitude of acceleration during the water-jet cutting process. This research is aimed at identifying the optimal technological conditions for the cutting process in terms of surface quality and cutting efficiency.

Based on the research, the following conclusions were made:

1. The amplitude of vibration acceleration varies and depends on both the specifics of the material being cut and the controllable technological parameters of the cutting process.
2. Small changes in technological parameters such as cutting speed v_{fi} and pressure p_i can lead to significant differences in the value of vibration acceleration amplitude.
3. During the analysis of the cutting process, three distinct and repeatable zones occurring during the cutting process were identified: the zone of entry of the water-water jet into the material of the cut workpiece, the zone of stabilization of the process (during full cutting) and the zone of exit of the jet from the cut material.
4. Regardless of the adopted technological parameters of pressure p_i and feed speed v_{fi}), the lowest values of acceleration were characterised by the process of cutting Al2024 aluminum alloy.
5. Significantly higher values of vibration acceleration amplitude (reaching up to 60 m/s^2) during cutting were registered for steel and titanium alloy for all zones and phases of the process (cutting zone, cutting zone and exit zones)
6. A nonlinear effect of the pressure value p_i and the feed motion speed v_{fi} on the value of vibration amplitude during the cutting process was observed.
7. In the case of steel cutting, an increase in pressure up to the limit of 300 MPa causes a linear increase in maximum accelerations (Figure 21) at each of the analysed feed speeds v_f. At the next pressure value of 350 MPa, there is a decrease in vibrations.

The conducted studies provide valuable cognitive conclusions, allowing for the assessment of cause-and-effect relationships between the amplitude of acceleration in the water-jet cutting process and the technological parameters of cutting. This information is indirectly beneficial for optimising the process and can significantly contribute to improving the efficiency and quality of cutting. As a result, it can lead to significant time savings in various cutting applications. By understanding how different technological parameters impact the vibration amplitudes, engineers and manufacturers can make informed decisions to enhance the overall performance and productivity of the water-jet cutting process.

Author Contributions: Conceptualization, M.L. and K.B.-U.; methodology, J.J.; software, M.L.; validation, J.J., M.L. and K.B.-U.; formal analysis, K.B.-U.; data curation, M.L.; writing—original draft preparation, M.L.; writing—review and editing, K.B.-U.; visualization, J.J.; supervision, J.J.; funding acquisition, M.L. All authors have read and agreed to the published version of the manuscript.

Funding: The activities of the Polish Metrological Union are financed from the funds of the Ministry of Education and Scienceas part of a targeted subsidy for the implementation of the task titled ”Establishment and Coordination of the activities of the Polish Metrological Union (PMU)” under contract no. MEiN /2021 /DPI/179.

Institutional Review Board Statement: Not applicable

Informed Consent Statement: Not applicable

Data Availability Statement: The data presented in this study are available on request from the corresponding author.

Conflicts of Interest: The authors declare no conflict of interest

References

1. Ficko, M.; Begic-Hajdarevic, D.; Cohodar Husic, M.; Berus, L.; Cekic, A.; Klancnik, S. Prediction of Surface Roughness of an Abrasive Water Jet Cut Using an Artificial Neural Network. *Materials* **2021**, *14*, 3108, doi:10.3390/ma14113108.
2. Bławucki, S.; Zaleski, K.; Leleń, M. Analysis of capabilities of cutting thin-walled structures of EN AW-2024 T351 alloy using an abrasive water-jet. *Mechanik* **2016**, 1078–1079, doi:10.17814/mechanik.2016.8-9.256.
3. Copertaro, E. Assessment of Resistive Strain Gauges Measurement Performances in Experimental Modal Analysis and Their Application to the Diagnostics of Abrasive Waterjet Cutting Machinery. *Measurement* **2022**, *188*, 110626, doi:10.1016/j.measurement.2021.110626.
4. Ochal, P.; Kuczmaszewski, J.; Kłonica, M. Assessment of surface finish quality of metal/composite compound structures as cut by abrasive water-jet. *Mechanik* **2017**, *90*, 436–438, doi:10.17814/mechanik.2017.5-6.59.
5. Moldovan, M.; Boşca, A.; Roman, C.; Prejmerean, C.; Prodan, D.; Bere, P.; Cosma, C.; Rotaru, H. Bone Reaction to a Newly Developed Fiber-Reinforced Composite Material for Craniofacial Implants. *Mater. Plast.* **2020**, *57*, 131–139, doi:10.37358/MP.20.2.5359.
6. Bere, P.; Dudescu, M.; Neamțu, C.; Cocian, C. Design, Manufacturing and Test of CFRP Front Hood Concepts for a Light-Weight Vehicle. *Polymers* **2021**, *13*, 1374, doi:10.3390/polym13091374.
7. Ganovska, B.; Molitoris, M.; Hosovsky, A.; Pitel, J.; Krolczyk, J.B.; Ruggierio, A.; Krolczyk, G.M.; Hloch, S. Design of the Model for the On-Line Control of the AWJ Technology Based on Neural Networks. *INDIAN J ENG MATER SCI* **2016**.
8. Bere, P.; Krolczyk, J.B. Determination of Mechanical Properties of Carbon/Epoxy Plates by Tensile Stress Test. *E3S Web Conf.* **2017**, *19*, 03018, doi:10.1051/e3sconf/20171903018.
9. Deaconescu, A.; Deaconescu, T. Response Surface Methods Used for Optimization of Abrasive Waterjet Machining of the Stainless Steel X2 CrNiMo 17-12-2. *Materials* **2021**, *14*, 2475, doi:10.3390/ma14102475.
10. Zagórski, I.; Kłonica, M.; Kulisz, M.; Łoza, K. Effect of the AWJM Method on the Machined Surface Layer of AZ91D Magnesium Alloy and Simulation of Roughness Parameters Using Neural Networks. *Materials* **2018**, *11*, 2111, doi:10.3390/ma11112111.
11. Müller, M.; Kolář, V.; Šulc, J.; Mishra, R.K.; Hromasová, M.; Behera, B.K. Effect of Waterjet Machining Parameters on the Cut Quality of PP and PVC-U Materials Coated with Polyurethane and Acrylate Coatings. *Materials* **2021**, *14*, 7542, doi:10.3390/ma14247542.
12. Löschner, P.; Jarosz, K.; Niesłony, P. Investigation of the Effect of Cutting Speed on Surface Quality in Abrasive Water Jet Cutting of 316L Stainless Steel. *Procedia Eng.* **2016**, *149*, 276–282, doi:10.1016/j.proeng.2016.06.667.
13. Biruk-Urban, K.; Bere, P.; Józwik, J.; Leleń, M. Experimental Study and Artificial Neural Network Simulation of Cutting Forces and Delamination Analysis in GFRP Drilling. *Materials* **2022**, *15*, 8597, doi:10.3390/ma15238597.
14. Maneiah, D.; Shunmugasundaram, M.; Raji Reddy, A.; Zareena Begum Optimization of Machining Parameters for Surface Roughness during Abrasive Water Jet Machining of Aluminium/Magnesium Hybrid Metal Matrix Composites. *Mater. Today Proc.* **2020**, *27*, 1293–1298, doi:10.1016/j.matpr.2020.02.264.
15. Copertaro, E.; Perotti, F.; Castellini, P.; Chiariotti, P.; Martarelli, M.; Annoni, M. Focusing Tube Operational Vibration as a Means for Monitoring the Abrasive Waterjet Cutting Capability. *J. Manuf. Process.* **2020**, *59*, 1–10, doi:10.1016/j.jmapro.2020.09.040.
16. Leleń, M.; Ruggiero, A.; Józwik, J. Geometric Features of a Multilayer Surface After Water Jet Cutting in Variable Cutting Conditions. *Manuf. Technol.* **2023**, *22*, 713–723, doi:10.21062/mft.2022.086.
17. Tyč, M.; Hlaváčová, I.M.; Barták, P. Analyses of Vibration Signals Generated in W. Nr. 1.0038 Steel during Abrasive Water Jet Cutting Aimed to Process Control. *Materials* **2022**, *15*, 345, doi:10.3390/ma15010345.
18. Wala, T.; Lis, K. Influence of Selected Diagnostic Parameters on the Quality of AWJ Cutting Surface. *Adv. Sci. Technol. Res. J.* **2022**, *16*, 129–140, doi:10.12913/22998624/144642.
19. Selvam, R.; Karunamoorthy, L.; Arunkumar, N. Investigation on Performance of Abrasive Water Jet in Machining Hybrid Composites. *Mater. Manuf. Process.* **2017**, *32*, 700–706, doi:10.1080/10426914.2016.1198039.

20. Adam Khan, M.; Gupta, K. Machinability Studies on Abrasive Water Jet Machining of Low Alloy Steel for Different Thickness. *IOP Conf. Ser. Mater. Sci. Eng.* **2020**, *709*, 044099, doi:10.1088/1757-899X/709/4/044099.
21. Józwik, J.; Ruggiero, A.; Leleń, M. Microscopic Analysis of the Surface Morphology of Multilayer Structures of the AluminumAlloy - Silicon Type after Water Jet Cutting. *Manuf. Technol.* **2023**, *22*, 693–702, doi:10.21062/mft.2022.076.
22. Monno, M.; Ravasio, C. The Effect of Cutting Head Vibrations on the Surfaces Generated by Waterjet Cutting. *Int. J. Mach. Tools Manuf.* **2005**, *45*, 355–363, doi:10.1016/j.ijmachtools.2004.07.010.
23. Xiu, C.; Weng, Y.; Shi, W. Vision and Vibration Data Fusion-Based Structural Dynamic Displacement Measurement with Test Validation. *Sensors* **2023**, *23*, 4547, doi:10.3390/s23094547.
24. Hreha, P.; Radvanská, A.; Hloch, S.; Peržel, V.; Królczyk, G.; Monková, K. Determination of Vibration Frequency Depending on Abrasive Mass Flow Rate during Abrasive Water Jet Cutting. *Int. J. Adv. Manuf. Technol.* **2015**, *77*, 763–774, doi:10.1007/s00170-014-6497-9.
25. Peržel, V.; Hreha, P.; Hloch, S.; Tozan, H.; Valíček, J. Vibration Emission as a Potential Source of Information for Abrasive Waterjet Quality Process Control. *Int. J. Adv. Manuf. Technol.* **2012**, *61*, 285–294, doi:10.1007/s00170-011-3715-6.
26. Tyč, M.; Hlaváčová, I.M.; Barták, P. Analyses of Vibration Signals Generated in W. Nr. 1.0038 Steel during Abrasive Water Jet Cutting Aimed to Process Control. *Materials* **2022**, *15*, 345, doi:10.3390/ma15010345.
27. Krenický, T.; Rimár, M. Monitoring of Vibrations in the Technology of AWJ. *Key Eng. Mater.* **2011**, *496*, 229–234, doi:10.4028/www.scientific.net/KEM.496.229.
28. Karmiris-Obratański, P.; Karkalos, N.E.; Kudelski, R.; Papazoglou, E.L.; Markopoulos, A.P. Experimental Study on the Correlation of Cutting Head Vibrations and Kerf Characteristics during Abrasive Waterjet Cutting of Titanium Alloy. *Procedia CIRP* **2021**, *101*, 226–229, doi:10.1016/j.procir.2020.11.011.
29. Kulisz, M.; Zagórski, I.; Korpysa, J. The Effect of Abrasive Waterjet Machining Parameters on the Condition of Al-Si Alloy. *Materials* **2020**, *13*, 3122, doi:10.3390/ma13143122.